# Effect of Integral Feedback on a Class of Uncertain Nonlinear Systems: Stability and Induced Limit Cycles

**Singith Abeysiriwardena**[1]
Mechanical and Aerospace Engineering Department,
University of Central Florida,
Orlando, FL 32816
e-mail: singith.abeysiriwardena@knights.ucf.edu

**Tuhin Das**
Mechanical and Aerospace Engineering Department,
University of Central Florida,
Orlando, FL 32816

*The theoretical problem addressed in the present work involves the effect of integral feedback on a class of uncertain nonlinear systems. The intriguing aspects of the problem arise as a result of transient constraints combined with the presence of parametric uncertainty and an unknown nonlinearity. The motivational problem was the state-of-charge (SOC) control strategy for load-following in solid oxide fuel cells (SOFCs) hybridized with an ultracapacitor. In the absence of parametric uncertainty, our prior work established asymptotic stability of the equilibrium if the unknown nonlinearity is a passive memoryless function. In contrast, this paper addresses the realistic scenario with parametric uncertainty. Here, an integral feedback/parameter adaption approach is taken to incorporate robustness. The integral action, which results in a higher-order system, imposes further restriction on the nonlinearity for guaranteeing asymptotic stability. Furthermore, it induces a limit cycle behavior under additional conditions. The system is studied as a Lure problem, which yields a stability criterion. Subsequently, the describing function method yields a necessary condition for half-wave symmetric periodic solution (induced limit cycle).* [DOI: 10.1115/1.4037837]

## 1 Introduction

In the present work, we have analyzed the closed-loop stability of a plant with an unknown nonlinearity. The effects of integral action to compensate for parametric uncertainty and the resulting third-order system are the main focus. The motivating problem to this theoretical development was operating solid oxide fuel cells (SOFCs) in load-following mode while preventing irreversible damages caused by fuel starvation [1–4]. This problem can be handled by regulating the fuel cell current on the basis of actual fuel flow [5,6], which is lagged by the fuel supply system (FSS) of the SOFC. However, for current regulation in the SOFC system, it has to be hybridized with an ultracapacitor. This necessitates control strategies to stabilize the hybrid fuel cell ultracapacitor system.

This problem was abstracted and posed in a generalized form in Ref. [7]. Analysis of the abstracted closed-loop system using Liénard equation proved asymptotic stability of the origin for all *first-third quadrant (passive) nonlinearities* [7–10]. However, in this prior work [7], an idealized system with no parametric uncertainty was considered. In this paper, we now consider a more realistic scenario with parametric uncertainty. A proportional-integral compensator is introduced by the addition of an integral feedback/parameter adaptation to the aforementioned abstracted system. The analysis is done on the arising third-order dynamics. Conditions for stability are derived by utilizing the absolute stability framework of the *Popov criterion*. Addition of the integral action is shown to impose further sector restriction on passive nonlinearities. Furthermore, in contrast to Ref. [7], which shows no possibility of limit cycle behavior for passive nonlinearities, the addition of an integral action is seen to induce limit cycle behavior. Consequently, we have explored the emergence of self-induced stable limit cycles using the *Describing function* technique [8], for passive odd nonlinearities. Similar studies on self-excited limit cycles, which consider known nonlinearities such as hysteretic systems, have been reported in Refs. [11–13].

This paper is organized as follows: First, a summary of the previous work on the state-of-charge (SOC) control strategy for load-following in SOFCs, hybridized with an ultracapacitor is provided [7]. Then, the problem of handling parametric uncertainty in the driven component of the driver-driven system is addressed through integral feedback. Subsequently, we analyze the emerging system and its stability using *Popov Criterion* by transforming the closed-loop system to a Lure problem. We also explore the emergence and necessary conditions for self-induced limit cycles. Finally, simulations are provided to justify and further explore the analysis performed.

## 2 Background

The issue of parametric uncertainty in the plant was recognized in Ref. [7]. However, the corresponding stability investigation was limited to a linearized analysis. Further research on parametric uncertainty based on nonlinear systems analysis is the focus of the present paper. Nevertheless, for the sake of refreshing knowledge, we present a summary of the previous work on the system.

**2.1 Motivating Example: Reformer-Based Solid Oxide Fuel Cells and Ultracapacitor System.** In this section, a brief background of the hybrid fuel cell energy system and the associated control problems is presented. A schematic of the hybrid SOFC system is shown in Fig. 1 [14]. The system consists of a fuel cell and an ultracapacitor that are connected in parallel to an electrical bus through direct current/direct current converters $C_1$ and $C_2$, respectively. Details of operation of the reformer-based SOFC system are available in Refs. [6] and [14]. The reformer reforms the fuel, methane with flow rate of $\dot{N}_f$, to a hydrogen-rich gas mixture that is used to deliver the current $i_{fc}$. The SOFC generates a steam-rich gas mixture as a by-product of current draw, of which a fraction ($k_c$) is

[1]Corresponding author.

Contributed by the Dynamic Systems Division of ASME for publication in the Journal of Dynamic Systems, Measurement, and Control. Manuscript received August 8, 2016; final manuscript received August 18, 2017; published online November 23, 2017. Assoc. Editor: Beshah Ayalew.

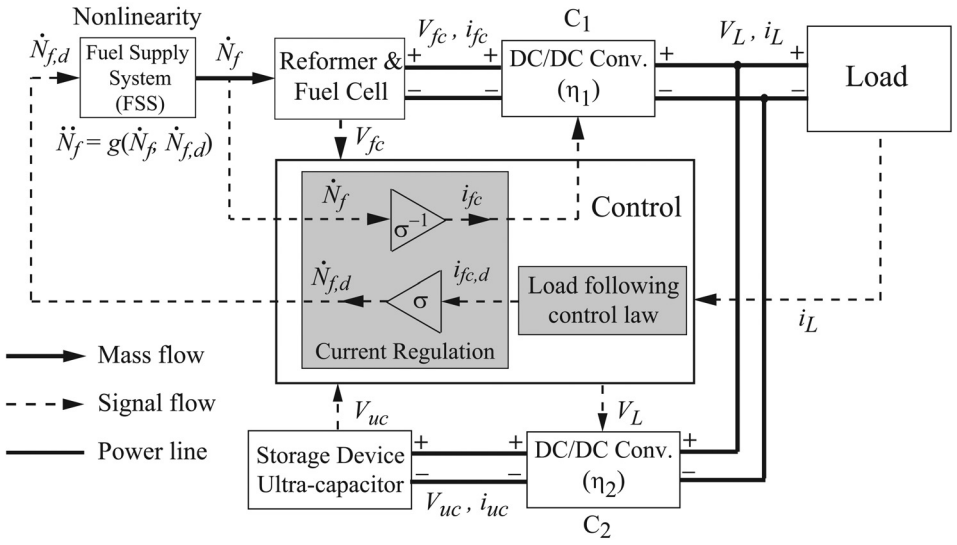


**Fig. 1 Schematic diagram of the hybrid SOFC system [5]**

recirculated to the reformer for providing steam for reforming. The converter $C_1$ provides unidirectional power flow and draws current $i_{\text{fc}}$ from the fuel cell, as commanded by the controller. $C_2$ is a bidirectional direct current/direct current converter that maintains a constant bus voltage $V_L$. The efficiencies of the converters $C_1$ and $C_2$ are represented as $\eta_1$ and $\eta_2$. It is also assumed that measurements of the fuel cell voltage $V_{\text{fc}}$, ultracapacitor voltage $V_{\text{uc}}$, load current $i_{L,}$ and actual fuel flow $\dot{N}_f$ are available to the controller. The variables $V_{\text{fc}}$, $V_{\text{uc}}$, and $i_L$ are readily measurable, and the measurement of $\dot{N}_f$ is available in FSS systems consisting of a fuel pump and/or valve. The controller generates two command signals, namely the demanded fuel flow $\dot{N}_{f,d}$ and $i_{\text{fc}}$. The general electrical power balance equation is expressed as

$$V_L i_L = \eta_1 V_{\text{fc}} i_{\text{fc}} + \eta_2 V_{\text{uc}} i_{\text{uc}} \tag{1}$$

The fuel cell is operated in a load-following mode. In this mode, the formulation of demanded fuel cell current $i_{\text{fc},d}$ is given by:

$$i_{\text{fc},d} = \frac{V_L i_L}{\eta_1 V_{\text{fc}}} - kE_s, \quad \text{where} \quad E_s = S - S_t \quad \text{and} \quad S = \frac{V_{\text{uc}}}{V_{\max}}, \quad S_t = \frac{V_{\text{uc},t}}{V_{\max}} \tag{2}$$

where $S$ is the instantaneous SOC of the ultracapacitor; $S_t$ and $V_{\text{uc},t}$ are the target SOC and target voltage, respectively; $V_{\max}$ is the maximum ultracapacitor voltage; and $k>0$ is a controller gain. Note that the efficiencies $\eta_1$ and $\eta_2$ are not readily measurable and although considered to be constant, may also slowly vary with time introducing a certain amount of uncertainty to Eq. (2). Counteracting this parametric uncertainty and its resulting effects on the system will be the central focus of the present paper.

For SOFCs, the dynamic limitations in load-following are manifested in the transient response of fuel utilization $U$. Fuel utilization is defined as the ratio of hydrogen consumption to the net available hydrogen in the anode [2]. Typically, 80–90% is set as the target range for optimal efficiency [2,3]. Constant fuel utilization ($U$) is a primary mode of operation of SOFCs [15–18], where the fuel flow is varied in conjunction with changes in power demand, to maintain $U$ at a set point (≈85%). However, SOFCs can be prone to hydrogen starvation at $U$ values of 80–90% due to delays in the FSS. The control strategy used to prevent fuel starvation by transient control of $U$ is summarized below. At steady-state $U$ has the form [6,14]

$$U = \frac{1 - k_c}{\left(4nF\dot{N}_f / i_{\text{fc}} \mathcal{N}_{\text{cell}}\right) - k_c} \tag{3}$$

where $i_{\text{fc}}$ is the fuel cell current, $\dot{N}_f$ is the fuel flow rate, $\mathcal{N}_{\text{cell}}$ is the number of cells in series, $F$ is Faraday's constant, $n=2$ is the number of electrons involved in each electrochemical reaction, and $k_c$ is the constant recirculation fraction. Rearranging Eq. (3), we obtain

$$\dot{N}_{f,d} = \frac{i_{\text{fc},d}\mathcal{N}_{\text{cell}}}{4nFU_{\text{ss}}}[1 - (1 - U_{\text{ss}})k_c] \Rightarrow \dot{N}_{f,d} = \sigma i_{\text{fc},d} \tag{4}$$

where $\sigma = \mathcal{N}_{\text{cell}}[1 - (1 - U_{\text{ss}})k_c]/4nFU_{\text{ss}}$. It is also noted that the dynamics of the FSS is considered unknown and nonlinear, and is represented by

$$\frac{d\dot{N}_f}{dt} = g\left(\dot{N}_f, \dot{N}_{f,d}\right) \quad \text{and} \quad \frac{d\dot{N}_f}{dt} = 0 \Rightarrow \dot{N}_f = \dot{N}_{f,d} \tag{5}$$

To compensate for delays along the fuel supply path, the current drawn from the fuel cell is regulated based on actual fuel flow $\dot{N}_f$, i.e.,

$$i_{\text{fc}} = \frac{4nFU_{\text{ss}}\dot{N}_f}{\mathcal{N}_{\text{cell}}} \frac{1}{[1 - (1 - U_{\text{ss}})k_c]} \Rightarrow i_{\text{fc}} = \sigma^{-1}\dot{N}_f \tag{6}$$

Next, we develop the equations of the overall feedback system shown in Fig. 1.

**2.2 Cascaded Configuration and the Generalized Feedback Structure.** In this section, we extract a cascaded feedback structure of the SOFC/UC hybrid system. The generic feedback structure we have used for our theoretical analysis relates to the practical example in the following manner. The driver part of the cascaded system, which includes the FSS dynamics, represents the unknown nonlinearity and the driven part represents the $E_S$ dynamics. The dynamic equations of $E_s$ and $i_{\text{fc}}$ are effectively in a cascaded connection [7], and the dynamics of $E_s$ is given by

$$\dot{E}_s = -\left(\frac{1}{CV_{\max}}\right)\left[\left(\frac{V_L i_L}{\eta_2 V_{\text{uc}}}\right) - \left(\frac{\eta_1 V_{\text{fc}}}{\eta_2 V_{\text{uc}}}\right) i_{\text{fc}}\right] \tag{7}$$

This connection, along with the load-following control law of Eq. (2), is shown in Fig. 2. The cascaded system consists of the

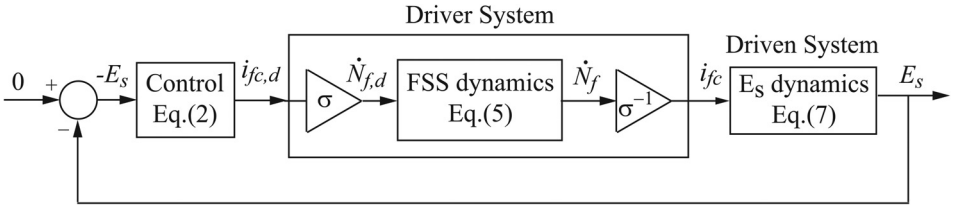


**Fig. 2 SOFC/UC hybrid as a cascaded system [5]**

unknown FSS dynamics acting as a driver system and the SOC dynamics acting as the driven system. It can be verified that the closed-loop system of Fig. 2 has a unique equilibrium at $i_{\text{fc}} = i_{\text{fc},d} = V_L i_L/(\eta_1 V_{\text{fc}})$, $E_s = 0$. This ensures that the closed-loop system addresses load-following and regulation of the ultra-capacitor's SOC simultaneously.

For a generalized treatment, the system in Fig. 2 is expressed as shown in Fig. 3. The mapping between the variables of Figs. 3 and 2 is

$$y \equiv i_{\text{fc}}, \quad r \equiv i_{\text{fc},d}, \quad x \equiv E_s, \quad \dot{x} = h_1 + h_2 y,$$
$$h_1 \equiv -\frac{1}{\eta_2}\left(\frac{V_L i_L}{C V_{\max} V_{\text{uc}}}\right), \quad h_2 \equiv \frac{\eta_1}{\eta_2}\left(\frac{V_{\text{fc}}}{C V_{\max} V_{\text{uc}}}\right) \tag{8}$$

The following assumptions were made in Ref. [7]:

(1) We assumed $e \triangleq (y - r) \to 0$ at steady-state and the nonlinearity satisfies:

$$\bar{f}(y,r) = -f(y-r) \equiv -f(e), \quad \Rightarrow \dot{y} = -f(e) \quad \text{and} \quad f(0) = 0 \tag{9}$$

This is not a restrictive assumption, as commonly occurring characteristics such as rate-limited, or saturation-based dynamics fall within this category, as shown in Ref. [19].

(2) In Ref. [7], $h_1$ and $h_2$ were treated as known constants, making the control law of Eq. (2)

$$r = -\frac{h_1}{h_2} - kx, \quad k > 0 \tag{10}$$

In Sec. 3, the restriction of $h_1$ and $h_2$ being known constants will be relaxed to a single unknown constant. The effect of this uncertainty, coupled with the unknown nonlinearity, is the main focus of the present paper.

Next, we summarize the approach adopted in Ref. [7] where parametric uncertainty was not considered. This motivates the work presented in the present paper.

**2.3 Prior Approach to Stability Analysis.** The problem statement of prior work in Ref. [7] is: Given the feedback system of Fig. 3 with the unknown nonlinear function $\bar{f}(y,r) = -f(e)$ as given in Eq. (9), determine conditions on $f(e)$, or category of functions $f(e)$, that yield a stable or an unstable equilibrium at $[x,e]^{\text{T}} = [0,0]^{\text{T}}$.

*2.3.1 Absolute Stability.* From Ref. [7], the closed-loop dynamic equations are

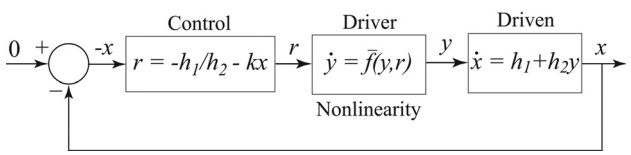


**Fig. 3 Generalized form of Fig. 2 [5]**

$$\dot{x} = -h_2 k x + h_2 e, \quad \dot{e} = -f(e) + k h_2 e - h_2 k^2 x \tag{11}$$

Applying the following coordinate transform, Eq. (11) can be written as:

$$z = e - kx, \quad \dot{z} = -f(e), \quad \dot{e} = -f(e) + k h_2 z \tag{12}$$

Eliminating the variable $z$, the system in Eq. (12) is expressed by

$$\ddot{e} + \frac{df}{de}\dot{e} + k h_2 f(e) = 0 \tag{13}$$

Equation (12) represents the coupled dynamics of $e$ and $z$ or equivalently $e$ and $x$. In carrying out a stability analysis of this system, the obvious issue is the lack of knowledge of the function $f(e)$. The approach was to consider classes of nonlinear functions $f(e)$ and to investigate their impact on the stability of the origin of the state space [7].

Stability of the origin of Eq. (12) was analyzed as a Lure problem [8,20]. The Lure problem considers the stability of an interconnection between a linear time invariant system with a memoryless nonlinearity. In formulating this problem, we expressed the dynamics of Eq. (12) by the structure in Fig. 4, which is mathematically equivalent to the system represented in Fig. 3.

The above formulation conforms to the structure of the Lure problem. It was observed that the sector condition $\psi \in [kh_2, \infty]$ guarantees absolute stability of the origin [7]. However, this sufficient condition is conservative and is evident from analysis using Liénard equations summarized next.

**2.4 Analysis as a Class of Liénard Equations.** The Liénard system refers to the following second-order nonlinear differential equation:

$$\ddot{\mu} + p(\mu)\dot{\mu} + q(\mu) = 0 \tag{14}$$

where $p(\mu)$ and $q(\mu)$ are two continuously differentiable functions of $\mu$ [9,10]. Under additional conditions on the functions $p(\mu)$ and $q(\mu)$, the Liénard equation has a unique and stable limit cycle, as described in detail in Refs. [7] and [9]. The following theorems were given to predict stability of Eq. (13), being a special case of Eq. (14) and Ref. [7].

THEOREM 1. *The class of Liénard equation Eq. (14), where $p(\mu) = \alpha(dq/d\mu)$, $q(\mu)$ is a continuously differentiable function such that $\mu\, q(\mu) > 0$, and $\alpha$ is a positive constant, has a globally asymptotically stable equilibrium at the origin $\mu = \dot{\mu} = 0$.*

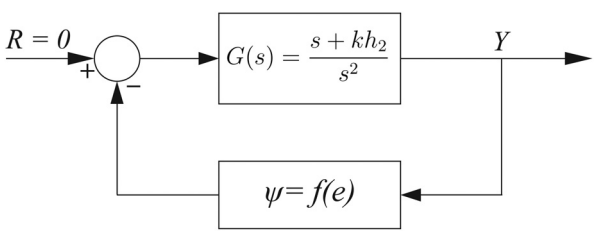


**Fig. 4 A Lure problem formulation derived from Fig. 3**

COROLLARY 1. *The feedback system of Fig. 3 with any unknown nonlinear function* $\bar{f}(y,r) = -f(e)$ *that satisfies* $f(0) = 0$, *and* $ef(e) > 0 \,\forall\, e \neq 0$, *has a globally asymptotically stable equilibrium point at* $e = \dot{e} = 0$.

The result of Corollary 1 is definitive compared to that in Sec. 2.3.1, as it establishes stable closed-loop performance for any passive memoryless function $f(e)$. A similar statement can be made for the generic feedback control of Eq. (10), without any additional sector or slope requirements on $f(e)$. It is noted from Eq. (11) that the equilibrium $e = \dot{e} = 0$ uniquely corresponds to $x = \dot{x} = 0$.

## 3 Parametric Uncertainty

**3.1 Problem Statement.** Given the feedback system of Fig. 3 with the unknown nonlinear function $\bar{f}(y,r) = -f(e)$ as given in Eq. (9), the work in Ref. [7] assumed that the controller has accurate knowledge of the values of parameters $h_1$ and $h_2$, appearing in the dynamic equation of the driven system. This is evident also from the control law of Eq. (10). Now, treating $h_1$ and $h_2$ as unknown parameters, we modify the control law to incorporate robustness to parametric uncertainty. Therefore, we investigate the impact of this change on the stability of the closed-loop system for the general class of passive memoryless nonlinearities.

**3.2 Robustness Via Integral Action/Parameter Adaptation.** Consider the feedback system of Fig. 3. Since $h_1$ and $h_2$ will now be treated as unknowns, the estimate of the combined parameter $(h_1/h_2)$ is used in the control law, as shown below:

$$r = -\hat{\beta} - kx, \quad k > 0, \quad \beta \triangleq \frac{h_1}{h_2} \tag{15}$$

where $\hat{\beta}$ represents the estimate of $\beta$. We define the estimation error

$$\mathcal{E} \triangleq (\beta - \hat{\beta}) \tag{16}$$

We propose the following integral update law for parameter estimation:

$$\dot{\mathcal{E}} = -\dot{\hat{\beta}} = -\gamma x \;\Rightarrow\; \mathcal{E} - \mathcal{E}_0 = -\gamma \int_0^t x\,dt, \quad \gamma > 0 \tag{17}$$

Treatment of $\beta$ as slowly varying is adequate for SOFCs subject to gradual changes in power demand. From Eqs. (8), (9), and (15)–(17) and noting that $e = (y - r)$, we deduce the following:

$$\dot{x} = h_2(\mathcal{E} + e - kx) = h_2 v, \quad v \triangleq \mathcal{E} + e - kx \tag{18}$$

and

$$\dot{e} = -f(e) + \gamma x + kh_2 v \tag{19}$$

Combining Eqs. (18) and (19), we obtain

$$\ddot{e} + \frac{df}{de}\dot{e} + kh_2 f(e) = -\gamma h_2 \int_0^t f(e)\,dt \tag{20}$$

The system representation is shown in Fig. 5 with integral action applied for parametric uncertainty. This effectively changes the prior control law in Fig. 3 to a PI compensator. Equation (17) is designed to make the resulting homogeneous equation in $x$ stable. This can be seen from differentiating Eq. (18) with respect to time and substituting for $\dot{\mathcal{E}}$ from Eq. (17), which yields

$$\dddot{x} + kh_2\ddot{x} + \gamma h_2 x = h_2\,\dot{e} \tag{21}$$

Comparing Eqs. (13) and (20), we see the addition of integral action to account for parameter uncertainty. However, it causes the closed-loop dynamics to be of third-order instead of second. By defining the variable $z = \int_0^t f(e)dt$, Eq. (20) can be expressed as

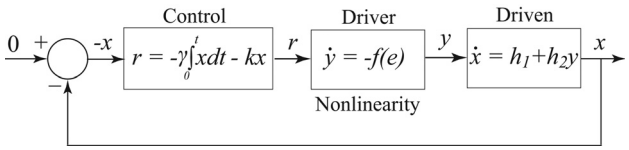


**Fig. 5 Generalized form of Fig. 3 with parametric uncertainty**

$$\dddot{e} + \frac{df}{de}\ddot{e} + kh_2 f(e) = -\gamma h_2 z, \quad \dot{z} = f(e), \quad \text{with} \quad z(0) = 0 \tag{22}$$

Since the function $f(e)$ is a passive memoryless function, the above system has a unique equilibrium at the origin $\dot{e} = e = z = 0$. Local stability of this origin can be analyzed using linearization. Since the linearization of $f(e)$ around the origin is $f(e) = \phi e$, $\phi > 0$, from Eq. (22), we have

$$\dddot{e} + \phi\ddot{e} + kh_2\phi\dot{e} + \gamma h_2\phi e = -\gamma h_2 \int_0^t \phi e\,dt$$
$$\Rightarrow \dddot{e} + \phi\ddot{e} + kh_2\phi\dot{e} + \gamma h_2\phi e = 0 \tag{23}$$

Using *Routh's Stability Criterion* [21], it can be shown that the necessary and sufficient condition for stability of the equilibrium $\dot{e} = e = z = 0$ for small perturbations is

$$k\phi > \gamma \tag{24}$$

The above analysis shows how the feedback gain $k$ and adaptive parameter gain $\gamma$ can be designed for the linear system represented by Eq. (23), and demonstrates that the adaptive approach taken to incorporate robustness has merit. However, further analysis must be conducted to study the performance of the robust controller in context of the nonlinear system. This analysis is presented next.

## 4 Nonlinear System Analysis

The discussion in Sec. 3.2 was focused on the linearized Eq. (23). For further analysis, we can pose Eq. (20) in its nonlinear form as

$$\dddot{e} + \frac{df}{de}\ddot{e} + \frac{d^2f}{de^2}(\dot{e})^2 + kh_2\frac{df}{de}\dot{e} + \gamma h_2 f(e) = 0, \quad \text{with} \quad f(0) = 0 \tag{25}$$

giving a third-order nonlinear equation of the closed-loop dynamics with robustness for parametric uncertainty. This follows reason as the addition of an integral action to the system for adaptive purposes would indeed increase the order of the system. The analysis of the dynamics of this third-order nonlinear equation, Eq. (25), gives more insight into the behavior of the closed-loop system.

**4.1 Absolute Stability.** We first look at the stability of the origin of Eq. (25) when analyzing the behavior of the closed-loop dynamics. Since the second-order case represented by Eq. (12) was mathematically equivalent to the structure of the Lure problem and $f(e)$ is still a passive memoryless nonlinearity, we can see that the third-order equation is also mathematically equivalent to the Lure problem [8,20]. We pose the closed-loop dynamics of Eq. (25) as

$$\begin{bmatrix} \dot{z}_1 \\ \dot{z}_2 \\ \dot{z}_3 \end{bmatrix} = \begin{bmatrix} 0 & 0 & 0 \\ 1 & 0 & 0 \\ kh_2 & \gamma h_2 & 0 \end{bmatrix} \begin{bmatrix} z_1 \\ z_2 \\ z_3 \end{bmatrix} + \begin{bmatrix} 1 \\ 0 \\ 1 \end{bmatrix} u, \quad y = \begin{bmatrix} 0 & 0 & 1 \end{bmatrix} \begin{bmatrix} z_1 \\ z_2 \\ z_3 \end{bmatrix}$$
$$u = -f(z_3),$$
$$z_3 = e \tag{26}$$

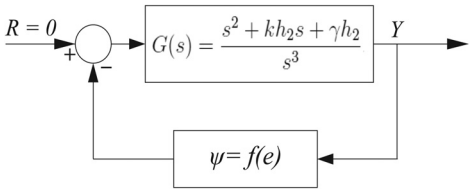


**Fig. 6 A lure problem formulation of third-order closed-loop dynamics**

Similar to Sec. 2.3.1, the resulting transfer function between $u$ and $y = e$ is given by

$$\frac{Y(s)}{U(s)} = G(s) = \frac{s^2 + kh_2 s + \gamma h_2}{s^3} \tag{27}$$

A premise of the Lure problem is that the matrices

$$\mathbf{A} = \begin{bmatrix} 0 & 0 & 0 \\ 1 & 0 & 0 \\ kh_2 & \gamma h_2 & 0 \end{bmatrix}, \quad \mathbf{B} = \begin{bmatrix} 1 \\ 0 \\ 1 \end{bmatrix}, \quad \mathbf{C} = [0 \quad 0 \quad 1] \tag{28}$$

form a controllable pair $(\mathbf{A}, \mathbf{B})$ and an observable pair $(\mathbf{A}, \mathbf{C})$. These conditions are satisfied in Eq. (28). Next, the system of Eq. (25) can be considered an interconnection of a linear and a nonlinear component, as shown in Fig. 6. The structure in Fig. 6 is mathematically equivalent to the system representation of Fig. 5.

The above formulation conforms to the structure of the Lure problem. Thereby, it allows direct application of the *Popov Criterion*, [8], to obtain a sector condition on $f(e)$ that will ensure stability of the feedback system in Fig. 6. From Theorem 7.3 of Ref. [8], we observe that the sector condition, $\psi \in [0, K_1]$, where $0 < K_1 \leq \infty$, will guarantee absolute stability of the origin of the feedback system if $Z(s) = (1/K_1) + (1 + s\gamma_1)G(s)$ is strictly positive real (SPR). Here, $\gamma_1$ is a constant such that $(1 + \lambda_k \gamma_1 \neq 0)$ for every eigenvalue $\lambda_k$ of $\mathbf{A}$. By Lemma 6.1 of Ref. [8], we know that $Z(s)$ is strictly positive real if $G(s)$ is Hurwitz and

$$\frac{1}{K_1} + \mathrm{Re}[G(j\omega)] - \gamma_1 \omega Im[G(j\omega)] > 0, \quad \forall \omega \in [-\infty, \infty] \tag{29}$$

By inspection, it is clear that the matrix $\mathbf{A}$ does not lead to a Hurwitz transfer function $G(s)$. Therefore, to compensate for this shortcoming and the required condition, we add and subtract the term $\alpha z_3$, where $\alpha > 0$ and define $\bar{\psi}(z_3) = f(z_3) - \alpha z_3$. This results in the Lure problem presented in Eqs. (26) and (27) being modified to

$$\begin{bmatrix} \dot{z_1} \\ \dot{z_2} \\ \dot{z_3} \end{bmatrix} = \begin{bmatrix} 0 & 0 & -\alpha \\ 1 & 0 & 0 \\ kh_2 & \gamma h_2 & -\alpha \end{bmatrix} \begin{bmatrix} z_1 \\ z_2 \\ z_3 \end{bmatrix} + \begin{bmatrix} 1 \\ 0 \\ 1 \end{bmatrix} u,$$
$$y = [0 \quad 0 \quad 1] \begin{bmatrix} z_1 \\ z_2 \\ z_3 \end{bmatrix}, \quad u = -\bar{\psi}(z_3), \quad z_3 = e \tag{30}$$

It is noted that the linear component in Eq. (30) retains controllability and observability. The modified transfer function between $u$ and $y = e$ is given by

$$\frac{Y(s)}{U(s)} = G(s) = \frac{s^2 + kh_2 s + \gamma h_2}{s^3 + \alpha s^2 + \alpha k h_2 s + \alpha \gamma h_2} \tag{31}$$

The condition for $G(s)$ being Hurwitz can be obtained by using the Routh–Hurwitz Criterion and is found to be

$$\alpha > \frac{\gamma}{k}$$

Now we go on to check the condition of the new $G(s)$ being SPR, which are the requirements to satisfy the condition given in Eq. (29). Since

$$G(j\omega) = \frac{(\gamma h_2 - \omega^2) + jkh_2\omega}{\alpha(\gamma h_2 - \omega^2) + j\omega(kh_2\alpha - \omega^2)}$$

we can define

$$P(\omega) = \frac{1}{K_1} + \mathrm{Re}[G(j\omega)] - \gamma_1 \omega \mathrm{Im}[G(j\omega)], \quad \forall \omega \in [-\infty, \infty]$$
$$P(\omega) = \frac{1}{K_1} + \frac{\alpha(\gamma h_2 - \omega^2)^2 + kh_2\omega^2(kh_2\alpha - \omega^2) - kh_2\gamma_1\alpha\omega^2(\gamma h_2 - \omega^2) + \gamma_1\omega^2(\gamma h_2 - \omega^2)(kh_2\alpha - \omega^2)}{\alpha^2(\gamma h_2 - \omega^2)^2 + \omega^2(kh_2\alpha - \omega^2)^2} \tag{32}$$

In the above equation, $K_1 > 0$ and the denominator of $P(\omega) > 0$. Now if the numerator of $P(\omega) > 0$, the condition of Eq. (29) will be satisfied and $Z(s)$ can be said to be SPR. Defining the numerator of $P(\omega)$ to be $N(\omega)$, we have

$$N(\omega) = \alpha(\gamma h_2 - \omega^2)^2 + (k^2 h_2^2 \alpha\omega^2 - kh_2\omega^4 - kh_2^2\gamma_1\gamma\alpha\omega^2 + kh_2\gamma_1\alpha\omega^4 + \gamma_1\omega^2(kh_2^2\gamma\alpha - (\gamma h_2 + kh_2\alpha)\omega^2 + \omega^4))$$
$$N(\omega) = \alpha(\gamma h_2 - \omega^2)^2 + \omega^2(\gamma_1\omega^4 - h_2(k + \gamma\gamma_1)\omega^2 + k^2 h_2^2\alpha) \tag{33}$$

from the terms of $N(\omega)$ in Eq. (33), it can be seen that $N(\omega) > 0, \quad \forall\omega$ can be guaranteed if the discriminant $(\Delta)$ of the quadratic function of $\omega^2$, $\gamma_1\omega^4 - h_2(k + \gamma\gamma_1)\omega^2 + k^2 h_2^2\alpha$ is negative. This gives us

$$\Delta = h_2^2(k + \gamma\gamma_1)^2 - 4k^2 h_2^2 \gamma_1 \alpha$$
$$= \gamma^2\gamma_1^2 + (2k\gamma - 4k^2\alpha)\gamma_1 + k^2 \tag{34}$$

Equation (34) gives another quadratic function of $\gamma_1$. The requirements of this quadratic function to have negative values for positive real values of $\gamma_1$ can be extracted from the value of the function at $\gamma_1 = 0$ and the value of its derivative at $\gamma_1 = 0$ as

$$2\alpha > \frac{\gamma}{k} \tag{35}$$

Now, if the discriminant of this function $(\Delta_1)$ is positive, $N(\omega)$ can be guaranteed to be positive for a range of real positive values of $\gamma_1$. Therefore

$$\Delta_1 = \left(2k\gamma - 4k^2\alpha\right)^2 - 4\gamma^2k^2 > 0$$
$$\Rightarrow \alpha > \frac{\gamma}{k} \tag{36}$$

By satisfying the condition in Eq. (36), the condition in Eq. (35) is also satisfied. Therefore, if $\alpha > (\gamma/k)$, by invoking *Popov criterion*, the nonlinear third-order system represented by Eq. (25) is absolutely stable if $\psi \in [0, \infty]$ implying $f \in [\alpha, \infty]$, where $\alpha$ can be arbitrarily small. This implication of the arbitrarily small $\alpha$ is that the condition $f(e) \to \infty$ as $e \to \infty$ is imposed upon $f(e)$, making $f(e)$ a $\mathcal{K}_\infty$ function. As a result of the earlier discussion, we state the following theorem.

THEOREM 2. *A system represented by Eq. (25) is absolutely stable if the nonlinear function f(e):*

- *Is a passive memoryless function* $f(0) = 0$, $ef(e) > 0$,
- *belongs to the sector* $f \in [\alpha, \infty]$, *where* $\alpha > (\gamma/k) > 0$, *and*
- *is a class* $\mathcal{K}_\infty$ *function.*

*If f(e) is not a* $\mathcal{K}_\infty$ *function and only satisfies* $f \in [\alpha, \infty]$ *on a set* $\mathbf{Y} \subset \mathbf{R}$, *then the foregoing conditions ensure that the system is absolutely stable with a finite domain.*

Now, as the sufficient condition for absolute stability of the third-order system arising from parametric uncertainty of the driver-driven system has been established, the next step is to investigate the behavior of the same system when unstable. The objective is to investigate the possibility of limit cycles induced by the introduction of an integral action to the compensator.

**4.2 Necessary Condition for Limit Cycle Behavior.** In this section, we analyze the system represented by Eq. (25) for the possibility of the existence of limit cycles when the system is unstable. Using the Lure problem formulation from Eq. (30), the possibility of a periodic solution of the output of the system $y = e$ is sought by representing the mentioned periodic solution by a Fourier series at a frequency $\omega$ and a set of Fourier coefficients that satisfy the system equation. The initial premise of *describing function method* leads to the solution of the *first-order harmonic balance equation* [8], obtained from

$$G(j\omega)\Psi(a) + 1 = 0 \tag{37}$$

where $\Psi(a)$ is the describing function of the nonlinearity $\psi = f(e)$ of the Lure's problem. It is obtained by applying a sinusoidal signal "$a \sin \omega t$" at the input of the nonlinearity and by calculating the ratio of the Fourier coefficients of the first harmonic at the output to $a$, the amplitude of the sinusoidal input to the nonlinearity. When dealing with describing functions of odd, time-invariant, memoryless nonlinearities, $\Psi(a)$ is a real value that is only dependent on $a$. Consequently, the imaginary part of Eq. (37) can be solved as the real equation

$$\begin{aligned} \mathrm{Im}[G(j\omega)] &= 0 \\ kh_2\alpha\omega(\gamma h_2 - \omega^2) - \omega(\gamma h_2 - \omega^2)(kh_2\alpha - \omega^2) &= 0 \\ \Rightarrow (\gamma h_2 - \omega^2)(kh_2\alpha\omega - kh_2\alpha\omega + \omega^3) &= 0 \\ \Rightarrow \omega = 0 \ \textit{or} \ \omega &= \sqrt{\gamma h_2} \end{aligned} \tag{38}$$

Considering the case of oscillations and ignoring $\omega = 0$, we are left with the probable frequency of oscillation as $\omega = \sqrt{\gamma h_2}$. Using this frequency, we can solve the real part of Eq. (37) as

$$1 + \Psi(a)\mathrm{Re}[G(j\omega)] = 0$$

determining the value of $\Psi(a)$ at $\omega = \sqrt{\gamma h_2}$

$$\Rightarrow 1 + \frac{kh_2(kh_2\alpha - \gamma h_2)\Psi(a)}{(kh_2 - \gamma h_2)^2} = 0$$
$$\Rightarrow \Psi(a) = \left(\frac{\gamma}{k} - \alpha\right)$$

Therefore, since the describing function $(\Psi(a))$ should be real and positive, for oscillations, a necessary condition would be

$$\Psi(a) > 0$$
$$\Rightarrow \frac{\gamma}{k} > \alpha \tag{39}$$

Note that this condition complements the condition for stability given in Eq. (36). While the condition given by Eq. (39) is only necessary but not sufficient, the satisfaction of this condition gives a probability of the unstable system exhibiting a limit cycle behavior at a frequency close to $\omega = \sqrt{\gamma h_2}$. The next step to determine a sufficient condition to move from a probable periodic solution to the certainty of a periodic solution for the system is to use the procedural method to determine the band of uncertainty in the exact version of the *harmonic balance equation* in consonance with Theorem 7.4 of Ref. [8]. While the criterion established in Eq. (39) is a property of the linear transfer function of the system represented by the Lure problem structure in Fig. 6, the band of uncertainty involves the specific properties of the nonlinearity. Thus, the mentioned procedure should be instigated on a system-by-system basis.

## 5 Simulations

To confirm the stability criterion presented in Theorem 2 and observe the behavior of the system when unstable, simulations are provided for the system represented by Eq. (25). Simulations and experimental results directly related to the SOFC/UC application showing the onset of instability and recovery therefrom can be found in Ref. [7]. For conciseness and generality, in this paper, we

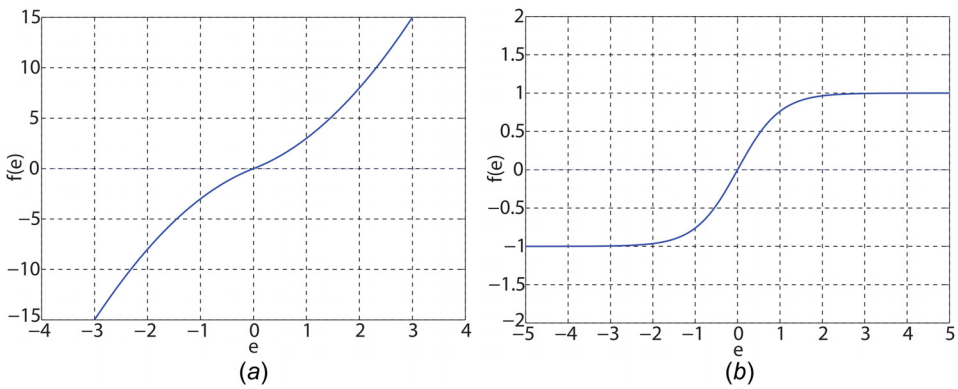


**Fig. 7 Nonlinear functions *f*(*e*): (*a*) correspond to Fig. 8(*b*) correspond to Figs. 9 and 10**

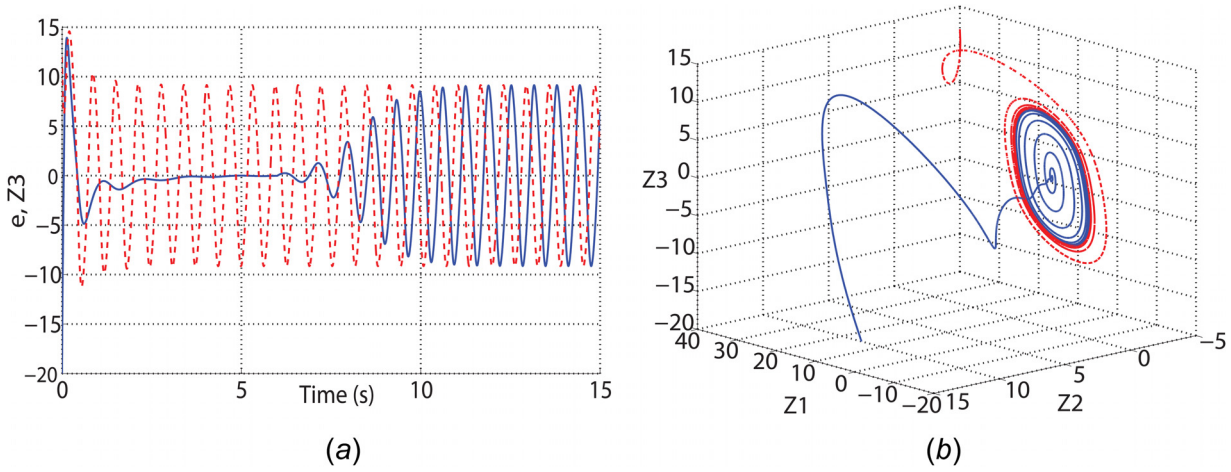


**Fig. 8 Effect of relative gains in inducing stable equilibrium or limit cycles**

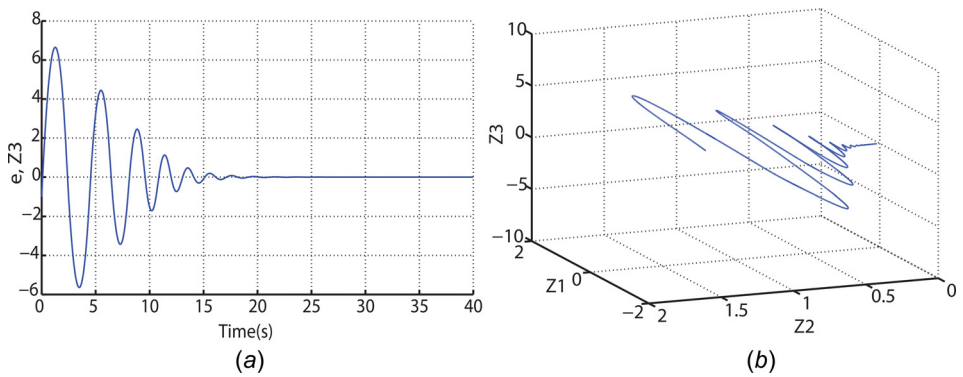


**Fig. 9 A non $\mathcal{K}_\infty$ nonlinearity yielding a locally stable equilibrium**

have considered a generalized example. The nonlinear functions $f(e)$ used are, first $f(e) = \text{sign}(e)e^2 + 2e$, a class $\mathcal{K}_\infty$ odd function plotted in Fig. 7(*a*). We note that $f(0) = 0$, $ef(e) > 0 \,\forall\, e \neq 0$ and $f(e) \in [1.5, \infty]$. The second function $f(e) = \tanh(e)$ is plotted in Fig. 7(*b*). It should be noted that although $f(0) = 0$, $ef(e) > 0 \,\forall\, e \neq 0$ but $f(e) = \tanh(e)$ is not a class $\mathcal{K}_\infty$ function.

We consider in Fig. 8 the largest allowable $\alpha = 1.5$, and $\gamma/k = 1$ (by setting both $\gamma = 1$ and $k = 1$). Hence, the equilibrium $\dot{e} = e = 0$ must be a globally asymptotically stable equilibrium, as predicted by Theorem 2. This is verified through the solid line plots for $t < 7$ in Figs. 8(*a*) and 8(*b*).

For $t \geq 7$, $\gamma$ is set to ten making $\gamma/k > \alpha$. As a result, the asymptotically stable behavior of the system becomes unstable, yet showing a limit cycle response indicated by the blue plot of Fig. 8(*a*). The accompanying blue plot of figure Fig. 8(*b*), shows the plot of all three states of the system ($[z_1, z_2, z_3]^{\mathrm{T}}$) first being asymptotically stable for $t < 7$ and diverging toward a limit cycle behavior when $t \geq 7$. The red plots in Figs. 8(*a*) and 8(*b*) represent a case where $\gamma/k > \alpha$ and the initial conditions ($[z_1, z_2, z_3]^{\mathrm{T}}$) are set in such a way that the system converges to the unique limit cycle shown above from the outside, instead of the inside as represented by the blue plots. It should be mentioned that the unique limit cycle to which the system converges in both cases is not planar but three-dimensional. Thus we, note that when the nonlinearity used is a $\mathcal{K}_\infty$ class function, the unstable system can result in a limit cycle behavior.

Next, we use $f(e) = \tanh(e)$ as the nonlinearity in Eq. (25) and set $\gamma/k = 0.1$. While the nonlinearity not being a class $\mathcal{K}_\infty$ function, the condition in Eq. (36) is still satisfied within a finite domain. Setting the initial conditions to be within the mentioned finite domain as $[z_1, z_2, z_3]^{\mathrm{T}} = [1, 1, -1]^{\mathrm{T}}$, the system still shows stable behavior as shown by Figs. 9(*a*) and 9(*b*). This shows the behavior of the same variables of the system as the corresponding plots in Fig. 8. Subsequently, we again set $\gamma = 10$ causing the initial conditions of ($[1, 1, -1]^{\mathrm{T}}$) to be outside the region where the function $f(e) = \tanh(e)$ satisfies the condition in Eq. (36), effectively violating the stability condition provided in Theorem 2. The resulting plot is shown in Fig. 10, where the response is unstable and unbounded. Again, it should be noted that when $f(e)$ is not a

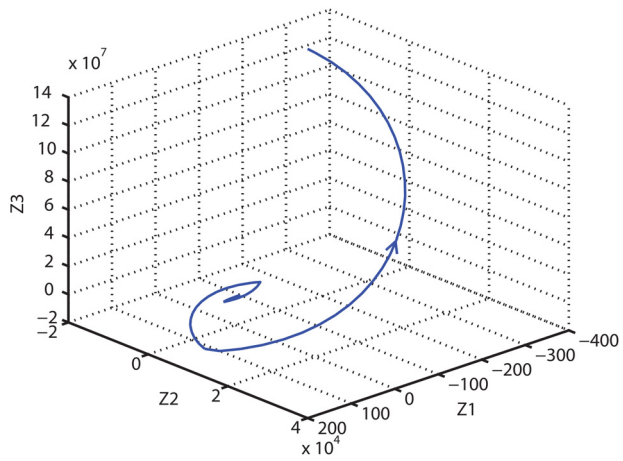


**Fig. 10 A non $\mathcal{K}_\infty$ nonlinearity yielding an unbounded response outside the region of attraction**

class $\mathcal{K}_\infty$ function, the unstable response is unbounded and does not show a limit cycle behavior, although the linear transfer function of the Lure problem structure satisfies the condition for probable limit cycle behavior given by Eq. (39).

## 6 Conclusion

The work presented in this paper extends from the theoretical work done on analyzing the closed-loop stability of a plant with an unknown nonlinearity. The motivating example behind the theoretical analysis was controlling an ultracapacitor's SOC in a hybrid SOFC system, by modulating the fuel cell's delivered power. The unknown nonlinearity is expressed in cascaded configuration in the plant dynamics. In previous work, analysis was done considering the generic system dynamics as a class of Liénard equations in the absence of parametric uncertainty. That analysis gave a definitive stability criterion and showed asymptotic stability of the origin for any passive memoryless nonlinearity. In the present work, the analysis has been extended to study the effects of parametric uncertainty on the closed-loop dynamics. The effects of robustness via integral feedback/parameter adaptation are explored through nonlinear dynamics of the resulting third-order system. In particular, sufficient conditions for stability, necessary conditions for the occurrence of induced limit cycles, or unbounded responses of the system are derived. These results show that integral action introduces restrictions on stability and induces limit cycles. Simulations are provided to demonstrate the efficacy of the developed theory.

## References


[1] Larminie, J., and Dicks, A., 2003, *Fuel Cell Systems Explained*, Wiley, Chichester, UK.

[2] Lazzaretto, A., Toffolo, A., and Zanon, F., 2004, "Parameter Setting for a Tubular SOFC Simulation Model," ASME J. Energy Resour. Technol., **126**(1), pp. 40–46.

[3] Sedghisigarchi, K., and Feliachi, A., 2002, "Control of Grid-Connected Fuel Cell Power Plant for Transient Stability Enhancement," IEEE Power Engineering Society Winter Meeting, New York, Jan. 27–31, pp. 383–388.

[4] Campanari, S., 2001, "Thermodynamic Model and Parametric Analysis of a Tubular SOFC Module," J. Power Sources, **92**(1–2), pp. 26–34.

[5] Das, T., and Weisman, R., 2009, "A Feedback Based Load Shaping Strategy for Fuel Utilization Control in Sofc Systems," American Control Conference (ACC), St. Louis, MO, June 10–12, pp. 2767–2772.

[6] Allag, T., and Das, T., 2012, "Robust Control of Solid Oxide Fuel Cell Ultracapacitor Hybrid System," IEEE Trans. Control Syst. Technol., **20**(1), pp. 1–10.

[7] Nowak, W., Geiyer, D., and Das, T., 2016, "Absolute Stability Analysis Using the Lie'nard Equation: A Study Derived From Control of Hybrid Fuel Cells," ASME J. Dyn. Syst. Meas. Control, **138**(3), p. 031007.

[8] Khalil, H., 2002, *Nonlinear Systems*, 3rd ed., Prentice Hall, Upper Saddle River, NJ.

[9] Davis, H. T., 2010, *Introduction to Nonlinear Differential and Integral Equations*, Dover Publications, Mineola, NY.

[10] Strogatz, S. H., 2001, *Nonlinear Dynamics and Chaos*, 1st ed., Westview Press, Boulder, CO.

[11] Esbrook, A., Tan, X., and Khalil, H. K., 2014, "Self-Excited Limit Cycles in an Integral-Controlled System With Backlash," IEEE Trans. Autom. Control, **59**(4), pp. 1020–1025.

[12] Yang, H., Jiang, B., and Cocquempot, V., 2010, *Fault Tolerant Control Design for Hybrid Systems*, Springer-Verlag, Berlin.

[13] Battistelli, G., Hespanha, J., and Tesi, P., 2012, "Supervisory Control of Switched Nonlinear Systems," Int. J. Adapt. Control Signal Process., **26**(8), pp. 723–738.

[14] Das, T., Narayanan, S., and Mukherjee, R., 2010, "Steady-State and Transient Analysis of a Steam-Reformer Based Solid Oxide Fuel Cell System," ASME J. Fuel Cell Sci. Technol., **7**(1), p. 011022.

[15] Stiller, C., Thorud, B., Bolland, O., Kandepu, R., and Imsland, L., 2006, "Control Strategy for a Solid Oxide Fuel Cell and Gas Turbine Hybrid System," J. Power Sources, **158**(1), pp. 303–315.

[16] Nehrir, M. H., and Wang, C., 2006, *Modeling and Control of Fuel Cells—Distributed Generation Applications*, Wiley, Hoboken, NJ.

[17] Murshed, A. M., Huang, B., and Nandakumar, K., 2010, "Estimation and Control of Solid Oxide Fuel Cell System," Comput. Chem. Eng., **34**(1), pp. 96–111.

[18] Gaynor, R., Mueller, F., Jabbari, F., and Brouwer, J., 2008, "On Control Concepts to Prevent Fuel Starvation in Solid Oxide Fuel Cells," J. Power Sources, **180**(1), pp. 330–342.

[19] Das, T., and Snyder, S., 2013, "Adaptive Control of a Solid Oxide Fuel Cell Ultra-Capacitor Hybrid System," IEEE Trans. Control Syst. Technol., **21**(2), pp. 372–383.

[20] Sastry, S., 1999, *Nonlinear Systems: Analysis, Stability and Control*, Springer-Verlag, New York.

[21] Franklin, G. F., Powell, J. D., and Emami-Naeini, A., 2014, *Feedback Control of Dynamic Systems*, 7th ed., Prentice Hall, Upper Saddle River, NJ.